

# FEATURE-EXTRACTION FROM LOCKIN-THERMOGRAPHY PHASE-IMAGES

Niels HOLTSMANN, Christian SPIESSBERGER, Andreas GLEITER and Gerd BUSSE  
INSTITUTE OF POLYMER-TECHNOLOGY, DEPARTMENT OF NON-DESTRUCTIVE  
TESTING (IKT-ZFP), UNIVERSITY OF STUTTGART,  
32 Pfaffenwaldring, Stuttgart 70569, Germany

## Abstract

Optically excited lockin-thermography (OLT) becomes increasingly popular since it is robust and easy to apply. However, the full potential of this method is not used, if only one lockin-frequency is evaluated. More information can be gained by correlating two or more measurements. This allows to gather information on features like the kind of defect, thickness of the specimen, properties of boundary layers, lateral heat flow etc. Certain defects are correlated to specific patterns in a scatter plot, akin to a fingerprint. Specimens with and without a certain feature can be distinguished more easily using suitable filters in the scatter plot. This is apparently of importance for automated defect detection and classification.

This paper covers feature-extraction using scatter plots. A wedge was used to measure the depth dependence of the phase angle for two lockin-frequencies. According to the thermal wave theory the scatter plot of the wedge shows a closed curve. Another specimen located next to the wedge contains flat bottom holes in different depths drilled from the rear side. The lateral heat flux near the holes results in a different shape of the correlated scatterplot curves, and therefore can be extracted from phase images in order to reveal hidden structures and defects.

## Introduction

In many cases it is advantageous to combine multiple NDE-methods in order to enhance the contrast between intact and defective parts. Correlation or data fusion merges results based on different physical effects into feature space, where the analysis is performed.

Classifying specimens by means of feature extraction has already been done at our institute several years ago [1]. Back then, the challenge was to distinguish between intact and defective rubber/metal elements. Neither mechanical eigenfrequencies nor dielectric characterization contained enough information for a clear decision. However, the combination of those two techniques clearly separates intact and defective parts (figure 1).

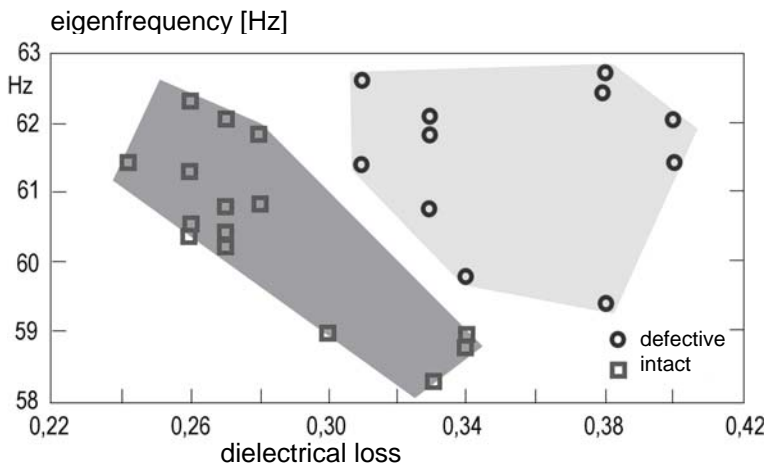


Figure 1: Separation of intact and defective parts in feature space [1].

These correlation techniques are also applicable to image based NDE-methods [2,3,4]. In order to correlate two or more images, the camera-specimen alignment has to be identical (or digitally merged).

This is not a problem for lockin thermography measurements, because multiple measurements can easily be done in identical alignment. Different lockin frequencies lead to different phase images, which can be correlated into scatter plots. Specimen properties - like for e.g. thickness variations - result in specific scatter plot patterns, akin to fingerprints.

This paper focuses on qualitative feature extraction from scatter plots and discusses advantages and applications of this technique.

## Theory

The complex amplitude of a thermal wave at the surface of a flat sample consisting of two layers with thickness  $L$  is given by [7,8]

$$\theta(L, f) = \frac{F_0}{4k\sigma} \left( \frac{(1+R)(1+Re^{-2\sigma L})}{1-R^2e^{-2\sigma L}} \right), \quad (1)$$

where  $F_0$  is a constant,  $k$  the thermal conductivity,  $R$  the thermal wave reflection coefficient of the rear sample surface and  $\sigma$  the complex wave number linked to the thermal diffusion length  $\mu$  by

$$\sigma = \frac{1+i}{\mu} = (1+i)\sqrt{\frac{\pi f}{\alpha}}, \quad (2)$$

with the lockin-frequency  $f$  and thermal diffusivity  $\alpha$ . The reflection coefficient  $R$  depends on the effusivities of the materials on both sides of the interface measured:

$$R = \frac{e_1 - e_2}{e_1 + e_2} \quad (3)$$

The phase value can be extracted from Eq. (1) using

$$\Phi = \arg(\theta(L, f)). \quad (4)$$

The phase has a characteristic dependence on sample thickness where frequency is a parameter (figure 2) [9].

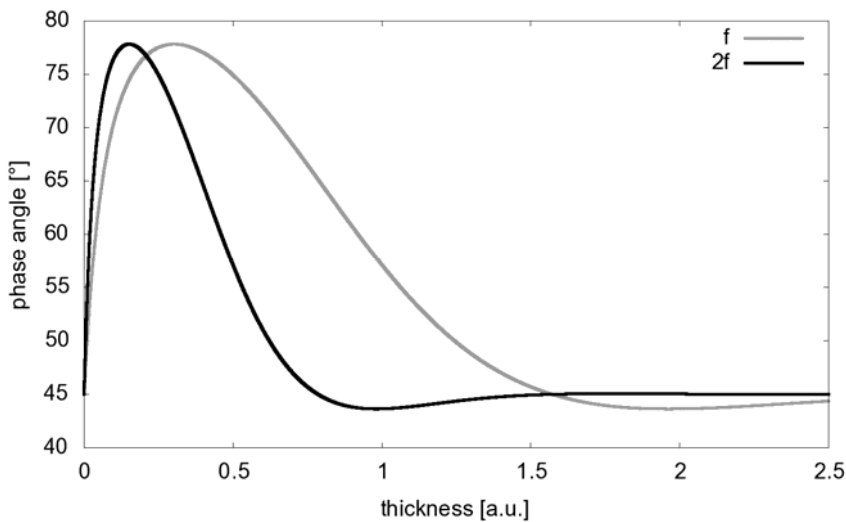


Figure 2: Phase angle in respect of thickness, plotted for two lockin-frequencies, one twice as high as the other

The reflection coefficient  $R$  at the measured boundaries significantly affects the phase contrast of lockin thermography. For the boundary solid / air  $R$  is almost 1, and almost  $-1$  when the thermal wave in a thermally insulating material hits a boundary to a good thermal conductor (e.g. polymer to aluminum). When  $R$  is close to zero the thermal wave is not reflected at all. The dependence of the phase curve on the reflection coefficient is plotted in figure 3 [10].

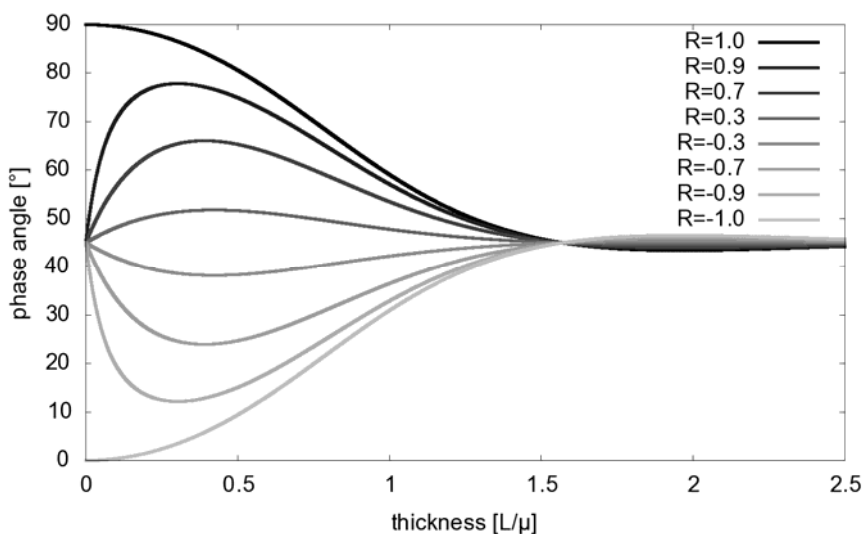


Figure 3: Phase in respect of thickness, plotted for various reflection coefficients, ranging from 1 to -1.

The schematical setup of optically excited lockin-thermography [11,12,13,14] is shown in figure 4. The thermal waves are generated at the sample surface by absorption of intensity modulated light, while an infrared camera remotely records the thermal emission on the surface. A pixelwise Fourier transformation of the stack of temperature images at the modulation frequency results in just two images, one displaying amplitude of local temperature modulation and the other one phase.

The phase shift between illumination and local temperature modulation at the surface depends on the local thermal properties of the sample. Therefore, the phase image, which is a map of the normalised delay of the thermal wave, reveals hidden boundaries and thermal features. An advantage of the phase image is its insensitivity to surface properties (e.g. varying emission

coefficients, surface topography) and to inhomogeneous heating due to non-uniform illumination. All these properties are suppressed in phase images due to internal normalisation of real to imaginary part performed by Fourier transformation [14].

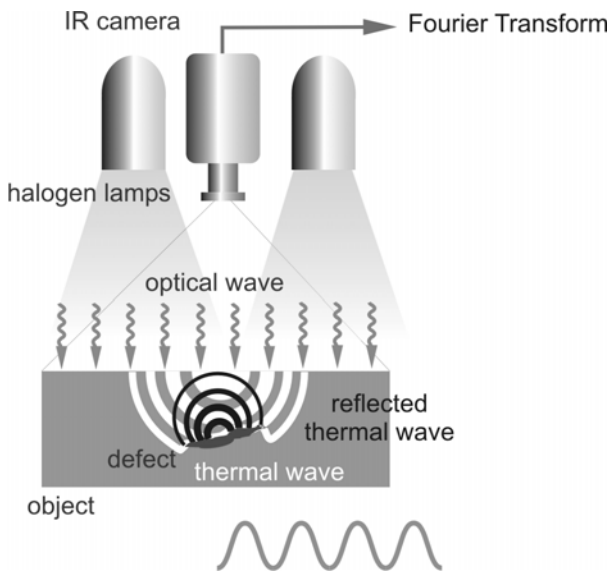


Figure 4: Schematical setup of a OLT-system

Our experimental equipment includes an infrared camera “Emerald” (CEDIP Infrared Systems, France) with an InSb-detector array of 640 x 512 pixels and an NETD of about 20 mK in the wavelength range 3 - 5  $\mu\text{m}$ . The heat source consists of four halogen lamps, each with up to 500 W electrical input power. The computer and the software “DisplayIMG” are from e/de/vis GmbH, Stuttgart.

### Data fusion of phase images

The dependence of phase on frequency contains additional information that is not accessible by measurements at just one frequency [5,6]. Therefore, it is beneficial to combine phase images within multi-dimensional scatter plots. The theoretical scatter plot for a wedge of homogeneous material and various reflection coefficients (figure 5) is an almost closed curve for a certain reflection coefficient. The lockin-frequency  $f_1$  for the first phase image is twice the frequency  $f_2$  of the second phase image. The curves were calculated with equations 1 and 4. Every thickness value with a certain reflection coefficient corresponds to one point in this plot.

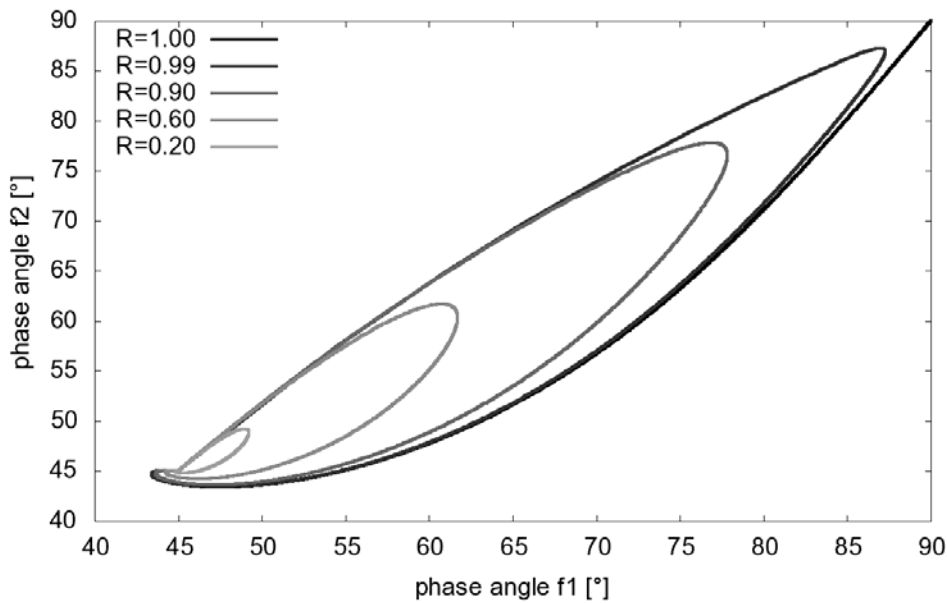


Figure 5: Data fusion of two phase values obtained at two different lockin-frequencies ( $f_1$  is twice  $f_2$ ) for reflection coefficients  $R$  ranging from 0.2 to 1.

The theory is confirmed by measurements on a polymer wedge which was milled into a rectangular plate (figure 6, top). Optically excited lockin thermography (OLT) measurements were performed at lockin-frequencies 0.1 Hz and 0.05 Hz (figure 6, bottom).

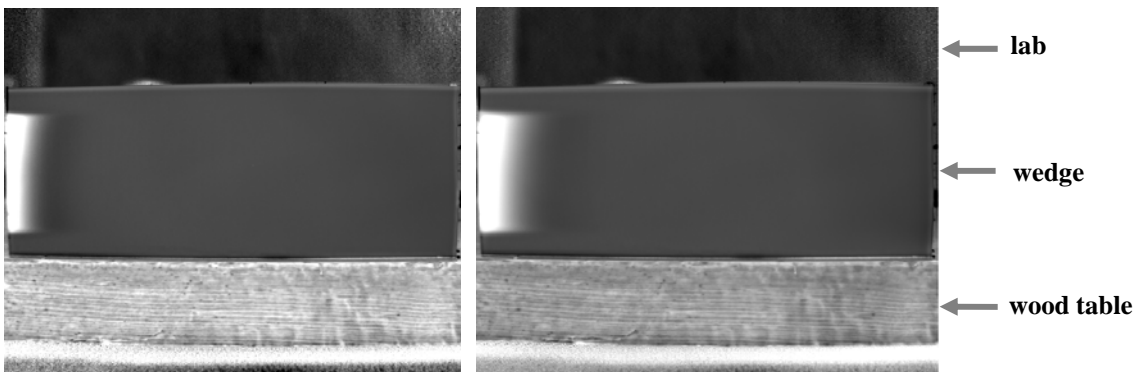
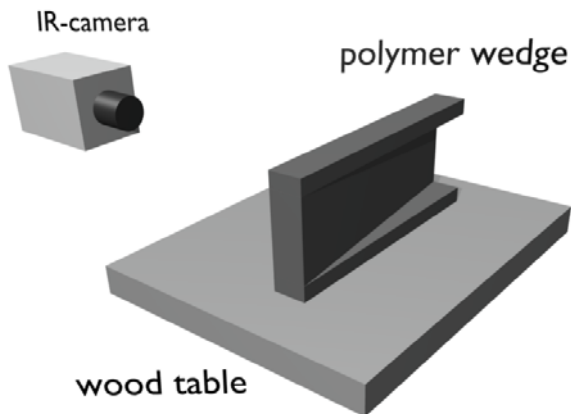


Figure 6: OLT-measurement setup with camera, wood table, and polymer wedge (top) and phase images of the wedge at 0.1 Hz (bottom left) and 0.05 Hz (bottom right).

In the white areas in figure 6 the lockin-frequency was low enough, so that the thermal wave could penetrate the sample. As the thermal diffusion length increases with decreasing frequency, the area is larger in the right image at 0.05 Hz modulation frequency.

The two phase images were then correlated by plotting the two phase angle data obtained for each pixel in a scatter plot plane (figure 7). The halogen lamps add a phase offset to the measured phase value, so that the measured correlation graph is not in the first but in the third quadrant. The cloud of data points obtained by correlating the two phase images displays several clusters and a curved line which matches the theoretical lines in figure 5. Therefore, this line represents the wedge. The clusters are caused by the background above the wedge and the wood table underneath.

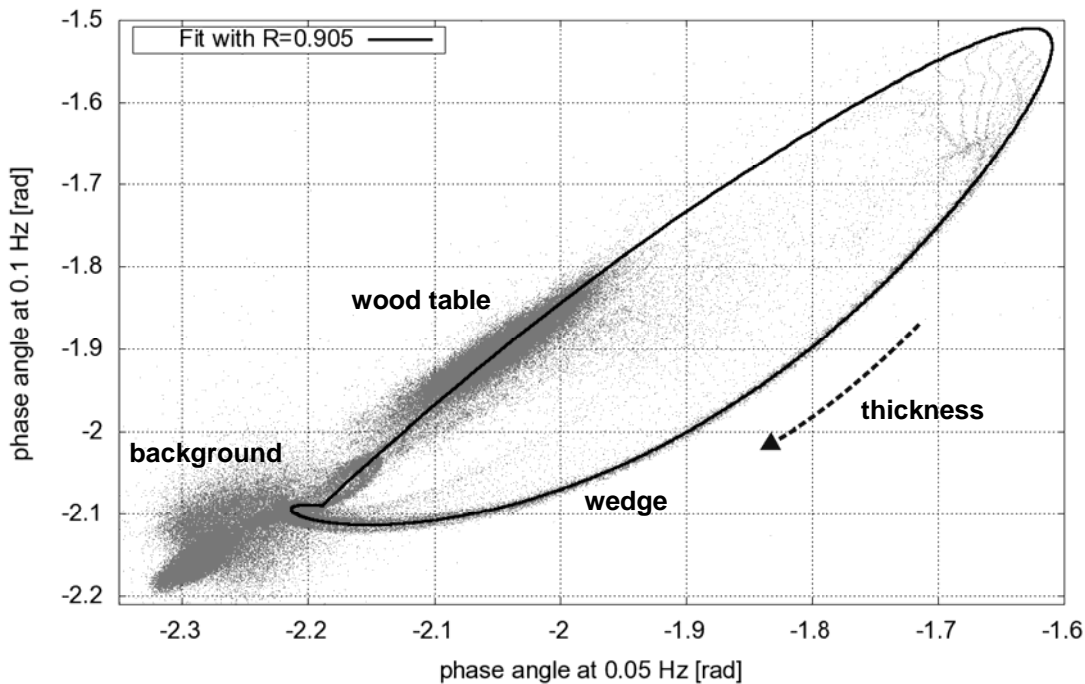


Figure 7: OLT-scatter plot: Phase data of the images shown in figure 5 plotted pixelwise against each other.

Such scatter plots are particularly suited for extracting meaningful features or parameters out of two (or multiple) physically different values. Therefore, it is much easier to extract thermal reflection coefficients and thicknesses out of scatter plots than out of phase images directly. The location of the pixel on the sample is temporarily lost. This information is not needed and might even be disturbing when thermal parameters need to be distinguished in order to characterize defects. Defects of the same thermal appearance might be located far from each other in the phase image while they might have the same phase coordinates in the scatter plot.

### Mapping lateral heat flows

The theoretical curves in figure 5 are based on the assumption of a wedge with one-dimensional heat flow. By suppressing all data points located on such curves, lateral heat flows can be imaged selectively.

Every point in the scatter plot represents certain thermal features, so backtracing certain areas to the original image can show their locations on the sample. This method is similar to spatial filtering in optical imaging methods where filtering in the Fourier plane allows for image processing and pattern recognition.

For demonstration purposes, the polymer wedge was positioned next to a sample provided with flat bottom holes drilled from the rear in different depths underneath the surface (hole 1 is nearest, hole 3 is farthest to the surface). Phase images were generated at 0.0250 Hz and 0.0125 Hz (figure 8).

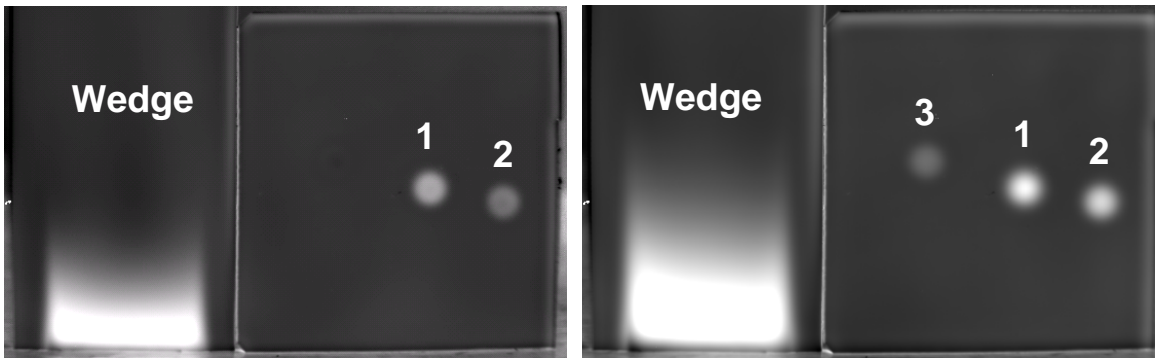


Figure 8: OLT phase images at 0.025 Hz (left) and 0.0125 Hz (right) of the polymer wedge and sample with flat bottom holes drilled from the rear.

Again, data fusion was performed in a two-dimensional plot (figure 9). The curved line of the wedge shows the ideal one-dimensional case. The three flat bottom holes are visible as curved branches in the middle of the image. Due to lateral heat flows, they cannot reach the ideal case of the one-dimensional wedge line.

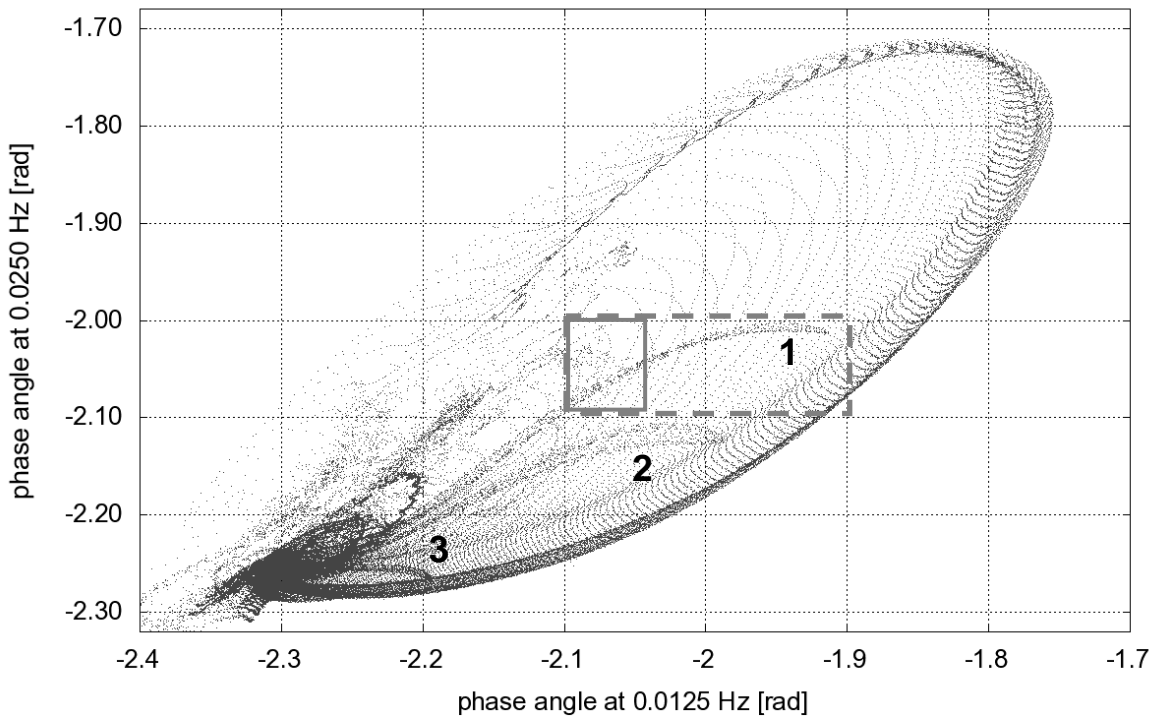


Figure 9: Scatter plot of the OLT phase images shown in figure 8.

The usefulness of the scatter plot for feature extraction can well be demonstrated on this example. The dashed rectangular area contains hole 1 including its edge effects plus a small part of the 1d wedge. Back inversion displays selectively the hole and a section of the wedge together with its edge effects (figure 10). The solid-framed area is far away from the curve, therefore filtering this area displays selectively lateral heat flows in a certain depth around hole 1 and along the wedge.

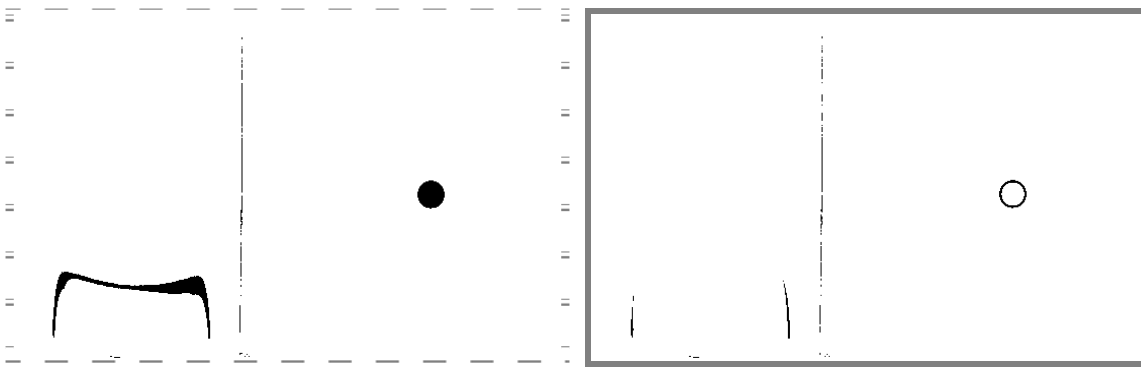


Figure 10: Feature extraction by filtering in the scatter plot of figure 9. The left image shows the data of the dashed area, the right image the data of the solid-framed rectangle.

## Conclusion

We have shown a new approach to determine certain thermal features like e.g. reflection coefficients by using lockin thermography. The basic idea is to combine two (or more) phase angle images taken at two different modulation frequencies. If the orientation of sample and camera with respect to each other is unchanged during the measurements, this method does not require corrections for the shape of the inspected sample.

The information derived from the scatter plot (e.g. hidden areas with lateral heat flow and flat areas) can be traced back to the initial image to display selectively certain features of hidden structures.

The data fusion of lockin thermography phase images by suitable filtering within scatter plots is obviously not confined to phase images of lockin thermography. It can also be applied to many other cases where image parameters have been changed or where images have been obtained that are based on different contrast mechanisms. Therefore, it can be a valuable tool in NDE, especially for automated defect detection and characterisation on production lines.

## References

- [1] L. Diener, P. Elsner, M. Ota, G. Busse, B. Brühl: Neuere Methoden der zerstörungsfreien Prüfung für Polymerwerkstoffe. Berlin: DVM, S. 261-276, 1990.
- [2] K. Tsukada, K. Hanasaki, X.E. Gros, Z. Liu: Experimenting with pixel level NDT data fusion techniques. IEEE Trans. Instrum. Meas., 49(5):1083-1090, 2000
- [3] G. Busse: Hybride Verfahren in der Zerstörungsfreien Prüfung (ZfP): Prinzip und Anwendungsbeispiele. In O.W. Geisler O.W. Buchholz, editor, Herausforderung durch den industriellen Fortschritt. Verlag Stahleisen GmbH, Düsseldorf, 2003.
- [4] J.P. Komorowski, K. Hanasaki, T. Kirubarajan, Z. Liu, D.S. Forsyth: Survey: State of the Art in NDE data fusion techniques. IEEE Transactions of Instrumentation and Measurement, 56, S. 2435-2451, 2007
- [5] C. Spiessberger, A. Gleiter, G. Busse: Merkmalsextraktion und Defektklassifizierung mit Lockin-Thermografie. MP Materials Testing 50 (2008), S. 632-639
- [6] C. Spiessberger, A. Gleiter, G. Busse: Data fusion of lockin-thermography phase images. Quantitative InfraRed Thermography Journal 6 (2009), im Druck
- [7] J. Jaarinen: Nondestructive Evaluation of Coatings by Low-Frequency Thermal Waves, Acta Polytechnica Scandinavica, Applied Physics Series No.162, 1988
- [8] A. Mandelis: Diffusion-Wave Fields, Springer-Verlag, 2001
- [9] G. Busse: Phase Angle Measurement for Probing a Metal, Appl. Phys. Lett. vol. 35, 1979, p. 759-760.
- [10] C.A. Bennett, R.R. Patty: Thermal wave interferometry: A potential application of the photoacoustic effect, Applied Optics vol. 21 1982, p. 49-54.
- [11] G.M. Carlomagno, P.G. Berardi: Unsteady thermography in nondestructive testing. Pro-ceedings of the 3rd Biannual Information Exchange, St. Louis/USA (1976), S. 33-39
- [12] J. L. Beaudoin, E. Merienne, R. Danjoux, M. Egge: Numerical system for infrared scan-ners and application to the subsurface control of materials by photo-thermal radiometry. Infrared technology and applications. SPIE 590 (1985), S. 287

- [13] P. K. Kuo, Z. J. Feng, T. Ahmed, L. D. Favro, R. L. Thomas, J. Hartikainen: Parallel thermal wave imaging using a vector lockin video technique. In: Photoacoustic and photothermal phenomena (Hrsg. P. Hess und J. Pelzl), Springer-Verlag, Heidelberg (1988), S. 415-418
- [14] G. Busse, D. Wu, W. Karpen: Thermal wave imaging with phase sensitive modulated thermography. J. Appl. Phys. 71 8 (1992), S. 3962-3965